

## DISCOVERY AND ORBITAL DETERMINATION OF THE TRANSIENT X-RAY PULSAR GRO J1750–27

D. M. SCOTT,<sup>1</sup> M. H. FINGER,<sup>1</sup> AND R. B. WILSON

Space Science Laboratory ES-84, NASA/Marshall Space Flight Center, Huntsville, AL 35812; scott@gibson.msfc.nasa.gov,  
 finger@gibson.msfc.nasa.gov, wilsonb@gibson.msfc.nasa.gov

D. T. KOH, T. A. PRINCE, AND B. A. VAUGHAN

Space Radiation Laboratory 220-47, California Institute of Technology, Pasadena, CA 91125;  
 koh@srl.caltech.edu, prince@srl.caltech.edu, brian@srl.caltech.edu

AND

D. CHAKRABARTY

Center for Space Research 37-561, Massachusetts Institute of Technology, Cambridge, MA 02139; deepto@space.mit.edu

Received 1997 March 20; accepted 1997 June 2

### ABSTRACT

We report on the discovery and hard X-ray (20–70 keV) observations of the 4.45 s period transient X-ray pulsar GRO J1750–27 with the BATSE all-sky monitor on board *CGRO*. A relatively faint outburst ( $< 30$  mcrab peak) lasting at least 60 days was observed during which the spin-up rate peaked at  $38 \text{ pHz s}^{-1}$  and was correlated with the pulsed intensity. An orbit with a period of 29.8 days was found. The large spin-up rate, spin period, and orbital period together suggest that accretion is occurring from a disk and that the outburst is a “giant” outburst typical of a Be/X-ray transient system. No optical counterpart has yet been reported.

*Subject headings:* pulsars: individual (GRO J1750–27) — X-rays: stars

### 1. INTRODUCTION

The first accretion-powered X-ray pulsar, Cen X-3, was discovered in 1971 with a pulse period of 4.8 s (Giacconi et al. 1971). Since that time, over 40 accretion-powered pulsars have been found (see, e.g., Bildsten et al. 1997; Nagase 1989). Their X-ray emission has exhibited two types of long-term behavior: either persistent (although variable) emission or transient outbursts lasting days to months. The transient outbursts occur either singly or in sets, recurring approximately with the orbital period and then possibly not occurring again for months to years (Priedhorsky & Holt 1987; Bildsten et al. 1997). We report on the discovery and observations of a new transient accretion-powered pulsar, GRO J1750–27, with the Burst and Transient Source Experiment (BATSE) on board the *Compton Gamma Ray Observatory* (*CGRO*). BATSE is a hard X-ray ( $> 20$  keV) all-sky monitor composed of eight identical uncollimated detector modules mounted on the corners of the spacecraft, and allows nearly continuous coverage of the entire sky except for that part blocked by the Earth (Fishman et al. 1989). GRO J1750–27 is the third of five new transient accretion-powered pulsars discovered using BATSE since the launch of *CGRO* in 1991 April (GRO J1008–57, Wilson et al. 1993; GRO J1948+32, Chakrabarty et al. 1995; GRO 2058+42, Wilson et al. 1995b; GRO J1744–28, Finger et al. 1996b). The number of known transients ( $\sim 30$ ) is now more than twice the number of known persistent pulsars (now 14). A comprehensive review of BATSE observations of accretion-powered pulsars can be found in Bildsten et al. (1997).

A single outburst from GRO J1750–27 was observed with BATSE approximately over the interval MJD<sup>2</sup> 49,915–49,978 (1995 July 17–September 18). A clear pulsa-

tion at a period of 4.45 seconds and period changes characteristic of an orbit and a significant intrinsic spin-up were observed, identifying this new source as an accretion-powered pulsar. The maximum pulsed flux was reached during MJD 49,940–49,945 (1995 August 11–16). No prior outburst from this source is apparent in the BATSE data over the interval MJD 48,362–49,914 (1991 April 16–1995 July 16), and no further outbursts have been observed through 1997 May 1. Below we report on the discovery, location, and orbital determination of GRO J1750–27.

### 2. DISCOVERY AND LOCATION

Pulsations with a 4.45 s period were discovered on 1995 July 29, coming from the Galactic center region as part of the BATSE all-sky pulsar monitoring program (Wilson et al. 1995b; Bildsten et al. 1997). On a daily basis Fourier power spectra are made with the 1.024 s resolution DISCLA data accumulated by each large area detector and inspected for the appearance of new or previously dormant pulsars. The sensitivity of this method allows the detection of sources down to a pulsed flux of  $\sim 20$ – $30$  mcrab in the 20–50 keV band on a 1 day timescale. Once detected, a more sensitive epoch-folding technique is used to monitor the pulse frequency.

The uncollimated nature of the BATSE large area detectors limits precise source localization, and the position of the pulsar was initially confused with that of another nearby nonpulsing transient, GRO J1735–27, located using the Earth occultation technique (Harmon et al. 1991; Zhang et al. 1993). The Earth occultation technique works best for bright persistent sources and can locate a source to  $\sim 0.1^\circ$ , but is useful only for sources brighter than  $\sim 100$  mcrab on timescales of 1 day or less. A second source location technique had been developed previously to locate weak pulsed sources (see Chakrabarty et al. 1995) and relies only on pulsed emission. Using this technique the pulsed

<sup>1</sup> Universities Space Research Association.

<sup>2</sup> MJD = Julian Date – 2,400,000.5.

source position was refined and was found to be inconsistent with the nonpulsed source. The pulsed source was designated GRO J1750–27 (Koh et al. 1995).

The pulsed source location method relies on the appearance of pulses in the DISCLA data from the large area detector when the source is not occulted by the Earth. For bright persistent sources, an Earth occultation step in the background count rate can be used to locate the source from the known position of the Earth's limb. For pulsed sources, a trial location is used to window the 20–50 keV DISCLA data, and the windowed data are fitted to a sinusoid with a variable frequency, amplitude, and phase to establish a maximum likelihood for that location. A grid of locations is then used to make a maximum likelihood map of the source location. The method improves in accuracy as more data are collected, as a result of both improved statistics and the changing occultation geometry caused by precession of the spacecraft orbit. A  $1^\circ$  by  $0.5^\circ$  error region (90% confidence) was established from data over the period MJD 49,930–49,958 (1995 August 1–29). This region was small enough that an *ASCA* target of opportunity was declared to search for the pulsar. A series of pointings with *ASCA* on MJD 49,985–49,986 (1995 September 25–26) detected a source located at  $\alpha(2000) = 17^{\text{h}}49^{\text{m}}12^{\text{s}}.0$ ,  $\delta(2000) = -26^\circ38'50''$  with an uncertainty of  $2'$  near the northwest corner of the BATSE error region. The clear presence of pulsations at a period of 4.452 s confirmed the source to be GRO J1750–27 (Dotani et al. 1995). An observation with *ROSAT* on MJD 49,996 (1995 October 6) refined the *ASCA* position to  $\alpha(2000) = 17^{\text{h}}49^{\text{m}}12^{\text{s}}.7$ ,  $\delta(2000) = -26^\circ38'36''$  with an uncertainty of  $4''$  (Dennerl & Trümper 1997). No star brighter than  $R \approx 17$  mag was found in the *ROSAT* error circle, and no optical counterpart has been reported as of 1997 May 1.

### 3. ORBITAL DETERMINATION

A pulse-timing study was conducted using the 20–50 keV channel of the 1.024 s time resolution DISCLA data type. Data were selected from source-facing detectors when the source was not occulted by the Earth assuming the celestial location given by Dotani et al. (1995). The data were filtered to remove occultation steps from bright sources, telemetry errors, spikes, high voltage off states, and other data contaminants. The times were corrected to the geocenter, and the data were linearly combined from different source-facing large area detectors with weights of the form

$$w_i = \frac{R_i}{\sum_i R_i^2}, \quad (1)$$

where  $R_i$  is the response for detector  $i$  calculated by folding a spectral model with the form  $\text{Flux}(E) = (B/E) \exp[-(E/kT)]$ , where  $E$  is energy in keV and  $B$  is a normalization factor, through the detector response matrices. A  $kT$  of 20 keV was used initially and later refined to 9.6 keV (see § 4).

A daily pulse frequency history was constructed using the combined DISCLA time series after removing a background model and correcting the times to the solar system barycenter using the JPL solar system ephemeris DE 200. The data were epoch-folded over a range of trial frequencies, and the trial frequency associated with the folded profile having the maximum  $\chi^2$  with respect to a fit to a constant flux was selected for each day. The background

model was a quadratic spline with an independent second derivative in rate fitted every 300 s.

A preliminary set of pulse-phase measurements was constructed next by utilizing the daily pulse-frequency history. An initial pulse-frequency model was obtained by fitting an orbital variation and a linear polynomial to the set of pulse frequencies obtained during the brightest portion of the outburst. A preliminary phase model, derived from the frequency model, was used to fold the DISCLA data over 1 day intervals. The pulse-folding technique is a harmonic-based method that models the pulses by fitting a harmonic series in pulse phase to 300 s segments of data. The harmonic series from the individual fitted segments are then combined on timescales of 1 day to produce a mean harmonic pulse profile. Details of the method can be found in Appendix B of Bildsten et al. (1997) and Finger, Harmon, & Wilson (1996a). Pulse-phase offsets were obtained by cross-correlating the folded profiles with a mean pulse template. The mean pulse template was obtained by combining all the data over the interval MJD 49,920–49,960 folded with an initial ephemeris such that phase offsets were reduced to less than 0.05 cycles. Because of the coarse sampling of the 4.45 s pulse period by the 1.024 s DISCLA bins, only three harmonic terms were used to represent the template and the folded pulse profile.

Changes in the pulse profile during the outburst might cause a systematic trend in the phase offsets unrelated to the intrinsic spin phase of the neutron star. No significant change in the pulse profile was detected during the course of the outburst on timescales greater than 2 days. The low signal-to-noise ratio of the pulse caused by the dimness of the outburst does not allow the detection of subtle changes in the profile, but any such changes, if present, would be expected to cause phase shifts smaller than the typical phase error of 0.03 cycles.

A refined phase model was constructed to extend the range of useful data to dimmer portions of the outburst. The orbital parameters were first improved by fitting an orbital model and a polynomial in pulse emission time to the initial phase history. The new trial orbital parameters were then fixed, and a second fit was performed using a quadratic spline phase model with frequencies given by:

$$v(t) = v_i + \dot{v}_i(t - t_i), \quad t_i \leq t < t_{i+1}, \quad (2)$$

where the interval duration  $t_{i+1} - t_i = \Delta t$  is constant for all intervals and  $t$  is the pulse emission time. The segmented phase model resulting from this two-step procedure was used to refold the data, including times beyond the range of the preliminary phase model. If the trend in the phase offsets continued beyond the edges of the preliminary phase model with sufficiently small errors, the data range was extended and a new fit performed. By repeating this procedure, a final set of phase measurements was obtained with errors of less than 0.1 cycle over the time interval MJD 49,915–49,978.

The final set of phase measurements, shown in Figure 1a, was fitted with an orbit relating the pulse emission time to the solar system barycentric pulse arrival time and polynomial phase model in pulse emission time. A seventh degree polynomial phase model resulted in a reduced  $\chi^2$  of 1.30 for 50 degrees of freedom. Phase models lower than seventh degree did not give acceptable fits, while higher order models did not significantly improve the fit. The total phase model is shown by the smooth curve in Figure 1a,

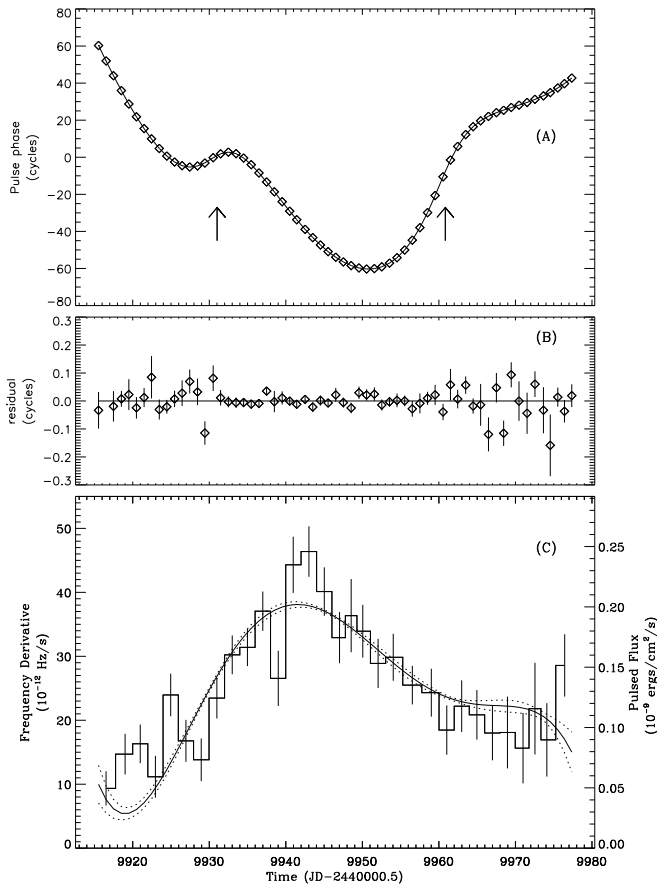


FIG. 1.—(a) Pulse phases relative to a model with a constant barycentric frequency of 0.224477 Hz. The phase model, discussed in the text, is the smooth curve and consists of an orbit plus a seventh-degree polynomial. The estimated time of periastron passage by the neutron star is marked by the arrows. (b) Residuals from the fit. (c) The barycentric spin-frequency derivative (scale on left) derived from the polynomial is given by the smooth curve. Errors are denoted by dashed line just above and below the curve. The pulsed flux (scale on right) averaged on 2 day intervals is given by the histogram.

while the fit residuals are displayed in Figure 1b. The resulting orbital parameters are given in Table 1. The spin frequency of the neutron star derived from the phase model is  $\nu(t) = 0.2244816(3) + 3.59(2) \times 10^{-8} t - 1.3(2) \times 10^{-13} t^2 - 2.3(1) \times 10^{-18} t^3 + 3.8(7) \times 10^{-23} t^4 + 1.0(2) \times 10^{-28} t^5 - 2.5(6) \times 10^{-33} t^6$  where  $\nu(t)$  is in hertz and  $t$  is the emission time measured in seconds since MJD 49,946.5 TDB. An orbital fit using the quadratic spline phase model was also tried but resulted in somewhat larger reduced  $\chi^2$  as well as being a less compact representation of the frequency history during the outburst.

A pulsed flux history was obtained by cross-correlating the folded profiles with a mean profile template with an rms

TABLE 1  
ORBITAL PARAMETERS OF GRO J1750 – 27

| Parameter                      | Symbol           | Value                                  |
|--------------------------------|------------------|--|
| Orbital period .....           | $P_{\text{orb}}$ | $29^{\text{d}}817 \pm 0^{\text{d}}009$ |
| Projected semimajor axis ..... | $a_x \sin i$     | $101.8 \pm 0.5 \text{ lt-s}$           |
| Eccentricity .....             | $e$              | $0.360 \pm 0.002$                      |
| Longitude of periastron .....  | $\omega$         | $206^{\circ}3 \pm 0^{\circ}3$          |
| Orbital epoch .....            | $T_p$            | JD 2,449,931.52 $\pm$ 0.01             |
| Pulsar mass function .....     | $f_x(M)$         | $1.24 \pm 0.02 M_{\odot}$              |

of unity and estimating a scaling factor. The pulse flux and spin-frequency derivative history are shown in Figure 1c as a histogram and smooth curve, respectively. Note that the pulsed flux and spin-frequency derivative are clearly correlated. Since the pulsed flux and spin-frequency derivative are determined independently, the observed correlation suggests that intrinsic and orbital changes in the pulse frequency have been successfully decoupled.

The relationship between the pulsed flux and the spin-frequency derivative was explored further by creating a set of discrete spin-frequency and pulsed flux values averaged over the same time intervals, which could then be fitted with various models and avoided possible systematic edge effects present in the polynomial torque model. The orbital parameters were fixed with the values given in Table 1, and the pulse phase was refitted using the quadratic spline phase model described earlier to produce a time history of the spin frequency. Time intervals near the beginning and end of the outburst were increased to improve the signal-to-noise ratio. The pulsed flux was averaged over these same time intervals. The two time histories are displayed in Figure 2. The bottom panel of Figure 2 shows a scatter plot of the pulsed flux versus spin-up rate. Neither a linear fit nor a power-law fit to the scatter plot was formally acceptable. At low flux levels the spin-up rate deviates from a power-law trend present at higher flux levels. By excluding the first three points in the outburst with spin-up rates less than 15

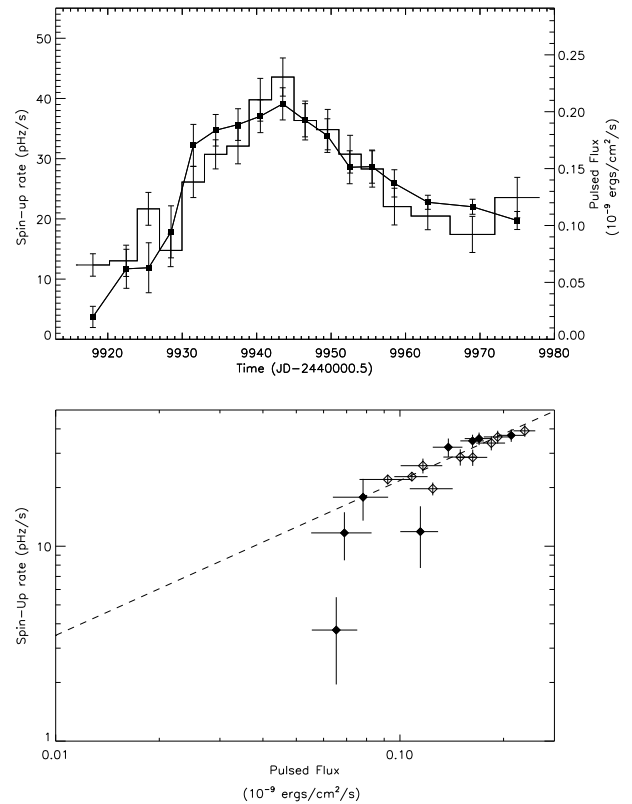


FIG. 2.—Spin-up rate vs. pulsed flux (20–50 keV) in GRO J1750–27. The top panel displays the outburst history of the spin-up rate (filled squares) and the pulsed flux (histogram) averaged over the same time intervals. The bottom panel is a scatter plot showing the strong correlation between the two histories. Points on the outburst rise (before 19942) are shown by filled diamonds and points on the outburst set by open diamonds. The dashed line is the best-fit power law excluding points with a spin-up rate less than 15  $\text{pHz s}^{-1}$ .

pHz s<sup>-1</sup>, a power-law fit of the form  $\dot{\nu} = A(f/f_p)^\alpha$  becomes acceptable with a reduced  $\chi^2$  of 1.05 for 12 degrees of freedom. Here  $\dot{\nu}$  is the spin-up rate (in pHz s<sup>-1</sup>),  $f$  is the pulsed flux, and  $f_p = 0.5$  is a prefixed pivot flux. Values of  $A = 78 \pm 8.7$  and  $\alpha = 0.79 \pm 0.1$  were obtained. Errors in both the pulsed flux and the spin-up rate were used in the fitting process. The power-law index is consistent with the value of  $\frac{6}{7}$  expected from simple models of the torque produced by disk accretion (e.g., Lamb, Pethick, & Pines 1973). The early outburst history may be evidence for the neutron star magnetospheric radius decreasing in size from the corotation radius. However, the detection of pulsations by GRO J1750–27 with *ASCA* 8 days after the last detection with BATSE on MJD 49,978 showed that the source was still accreting and that the magnetosphere did not rapidly exceed the corotation radius just after dropping below the BATSE detection threshold. More sensitive observations of future outbursts will be needed to determine the spin-up rate/flux relationship in the important faint-luminosity regime.

#### 4. PULSE PROFILE AND X-RAY SPECTRUM

A pulse profile and X-ray spectrum were constructed from 127 ms time-resolution data specifically collected for GRO J1750–27 during the outburst using the pulsar data mode (Fishman et al. 1989). Data with 16 energy channels from the BATSE large area detector most nearly facing the source were used in this analysis. A segmented quadratic spline phase model combined with an orbital model using the parameters given in Table 1 was used to epoch-fold the data over the time span MJD 49,960–49,967.5 (1995 August 31.0–September 7.5). The pulse profile obtained in the 20–70 keV range is shown in Figure 3. The broad pulse is comparable to the profiles in transient Be systems, such as GRO J1008–57 (Wilson et al. 1993). A spectral fit was also made to these data by folding through the detector response trial spectra of the following form:

$$\text{Flux}(E) = A(E_p/E) \exp [-(E - E_p)/kT], \quad (3)$$

where  $E$  is energy in keV,  $E_p$  is a pivot energy which was fixed at 30 keV, and  $A$  is a normalization factor. Since off-source background measurements cannot be obtained using the BATSE large area detectors, only a pulsed spectrum was constructed using the difference between the on-

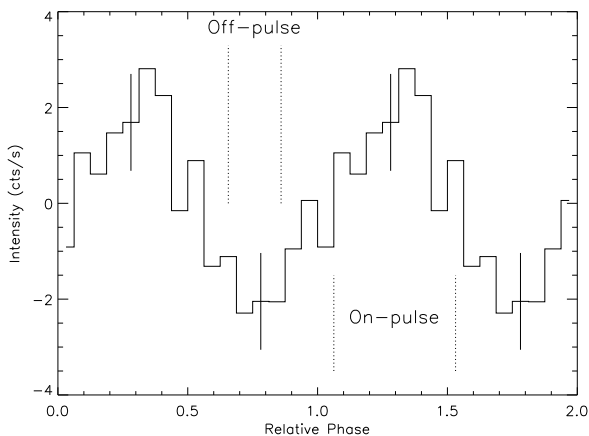


FIG. 3.—Pulse profile folded from 127 ms time-resolution data. The off and on pulse-phase intervals were used to construct a pulsed intensity spectrum.

pulse and off-pulse intervals defined in Figure 3. The resultant model parameters are  $A = (2.28 \pm 0.45) \times 10^{-4}$  photons cm<sup>-2</sup> s<sup>-1</sup> and  $kT = 9.6 \pm 2.9$  keV. The integrated pulsed intensity in the 20–70 keV band is  $(2.98 \pm 0.074) \times 10^{-10}$  ergs cm<sup>-2</sup> s<sup>-1</sup>.

#### 5. DISCUSSION

An optical counterpart has not been reported yet for GRO J1750–27, so the system type is unknown. However, the measured pulse and orbital periods place GRO J1750–27 squarely among the Be systems on a pulse period/orbital period plot (i.e., a Corbet diagram; see Corbet 1986; Waters & van Kerkwijk 1989). Empirically, only Be systems have been found in this region of the Corbet diagram, which strongly suggests that the optical counterpart is a Be star. We also note that the pulse period and orbital parameters of GRO J1750–27 are very similar to those of the Be/X-ray binary V0332+53 (Stella et al. 1985).

X-ray outbursts from the Be transients can be roughly divided into two types: “normal” and “giant” (Motch et al. 1991) or, equivalently, class I and class II (Stella, White, & Rosner 1986). The “giant” outbursts are bright, and substantial spin-up of the pulsar occurs (with observed  $\dot{\nu}$  of 5–40 pHz s<sup>-1</sup> at outburst peak; Bildsten et al. 1997). In contrast, the normal outbursts are much fainter (peak flux <20% of giant outburst peak), while the pulsar either shows little to no spin-up or exhibits spin-down (see Finger et al. 1996a for examples of these behaviors in A0535+262). The very large spin-up rate observed (38 pHz s<sup>-1</sup> at peak) suggests that the outburst from GRO J1750–27 may be classified as a “giant” outburst and that accretion is occurring from a disk. As in the “giant” outbursts observed in other Be systems (e.g., Finger et al. 1996a; Parmar et al. 1989), the spin-up rate during the outburst of GRO J1750–27 is correlated with the pulsed flux.

The large spin-up rate observed and the short spin period of GRO J1750–27 together suggest a peak luminosity during the outburst exceeding  $1 \times 10^{38}$  ergs s<sup>-1</sup>. If one assumes that disk accretion is occurring and that all the specific angular momentum of the accreting material is added to the neutron star at the magnetospheric radius  $r_m$ , then the torque  $N_m$  experienced by the neutron star is given by  $N_m = \dot{m}(GM_x r_m)^{1/2}$ , where  $G$  is Newton’s constant of gravitation and  $M_x$  is the neutron star mass. The observed torque is given by  $N_{\text{obs}} = 2\pi I \dot{\nu}$ . In order to keep the propeller effect from preventing accretion onto the neutron star, the magnetospheric radius  $r_m$  must be less than the corotation radius  $r_{\text{co}} = (GM_x/4\pi^2)^{1/3} \nu^{-2/3}$ , where  $\nu$  is the spin frequency of the pulsar. Setting  $r_m = r_{\text{co}}$ , we find that the maximum torque for a given mass accretion rate must be less than

$$N_{\text{max}} \leq \dot{m}(GM_x)^{2/3} (2\pi\nu)^{-1/3}. \quad (4)$$

Since  $N_{\text{obs}} \leq N_{\text{max}}$ , we find upon substituting  $N_{\text{obs}}$  into equation (4) and rearranging terms that

$$\dot{m} \geq I(4\pi^2/GM_x)^{2/3} \nu^{1/3} \dot{\nu}_{\text{obs}}, \quad (5)$$

or in more convenient units,

$$\dot{m}_{17} \geq 0.444 \nu^{1/3} \dot{\nu}_{\text{obs}} I_{45} M_x^{-2/3}, \quad (6)$$

where  $\dot{m}_{17}$  has units of  $10^{17}$  g s<sup>-1</sup>,  $\dot{\nu}_{\text{obs}}$  is in pHz s<sup>-1</sup>,  $I_{45}$  has units of  $10^{45}$  g cm<sup>2</sup>, and  $M_x$  is in solar masses. If we let

$M_x = 1.4$ ,  $I_{45} = 1$ , and take the measured values of  $\nu = 0.22462$  Hz and  $\dot{\nu} = 38$  pHz s<sup>-1</sup>, we find that  $\dot{m}_{17} \geq 8.2$  at the peak of the outburst. The bolometric luminosity can be estimated using  $L_{\text{bol}} = (GM_x/R_x)\dot{m}$  as  $1.5 \times 10^{38}$  ergs s<sup>-1</sup> or larger using the canonical neutron star parameters assumed above and complete efficiency in converting gravitational potential into radiation which appears mostly in the X-ray energy band. The outburst thus appears to be very bright, with a luminosity comparable to the Eddington luminosity of  $L_{\text{Edd}} = 1.8 \times 10^{38}$  ergs s<sup>-1</sup> for spherical accretion onto a  $1.4 M_\odot$  neutron star.

The distance to GRO J1750–27 can be estimated using the bolometric flux at the observer's position and the source luminosity. From the observed pulsed flux, the bolometric mean flux over the pulse is given by  $F_{\text{mean}} = BF_{\text{pulsed}}/f_p$ , where  $B$  is a bolometric correction and  $f_p$  is a pulsed fraction defined as the ratio of the pulsed flux to the mean flux (pulsed + unpulsed). The distance can thus be estimated as  $d = (\beta L_{\text{bol}}/4\pi F_{\text{mean}})^{0.5}$ , where  $\beta$  is a factor accounting for the beaming. The beaming factor in this case is the ratio of the mean pulsed flux to the flux from the source averaged over  $4\pi$  sr and is equal to 1 for an isotropically emitting source. The broad pulse profiles observed from most accretion-powered pulsars (Bildsten et al. 1997) and GRO J1750–27 imply broadly beamed emission patterns and hence  $\beta > 1$  on the average. It is possible that the faintness of the GRO J1750–27 outburst is the result of unfavorable beaming and hence  $\beta < 1$  in this case. We will conservatively assume  $\beta = 1$ , which should result in an underestimate of the distance if the emission pattern does not produce a large per-

centage of unobserved beamed flux. The bolometric correction and pulsed fraction are unknown, but for illustrative purposes we assume values of 3.0 and 0.3 respectively, based upon observations of other Be/X-ray binary systems (see, e.g., Bildsten et al. 1997). Using the value for  $F_{\text{obs}}$  given in § 4 and adopting a source luminosity of  $\sim 1 \times 10^{38}$  ergs s<sup>-1</sup> appropriate for the time interval of the flux estimate, we derive a distance of approximately 18 kpc to GRO J1750–27. This distance estimate and a location on the celestial sphere near the Galactic center place GRO J1750–27 well on the opposite side of the Milky Way from the Sun, indicating that most if not all giant outbursts from Be/X-ray binaries within the Galaxy are detectable with the BATSE large area detectors. In the 5 years since the launch of CGRO, a total of about 10 giant outbursts have been observed from various Be/X-ray binaries (Bildsten et al. 1997). Given the systematic uncertainties in the distance estimate to GRO J1750–27, we can make the conservative assumption that BATSE is sensitive enough to detect all giant outbursts in at least half of the Milky Way. Thus we can estimate a total giant outburst rate of  $\sim 2\text{--}4$  yr<sup>-1</sup> in the Galaxy.

This work was supported in part by the National Aeronautics and Space Administration (NASA) under grants NAG 5-3293 and NAG 5-1458. D. C. was supported by a NASA Compton GRO Postdoctoral Fellowship under grant NAG 5-3109. We also thank the anonymous referee for useful comments.

#### REFERENCES

- Bildsten, L., et al. 1997, ApJS, in press  
 Chakrabarty, D., Koh, T., Bildsten, L., Prince, T. A., Finger, M. H., Wilson, R. B., Pendleton, G. N., & Rubin, B. C. 1995, ApJ, 446, 826  
 Corbet, R. H. D. 1986, MNRAS, 220, 1047  
 Dennerl, K., & Trümper, J. 1997, A&A, in press  
 Dotani, T., Fujimoto, R., Nagase, F., & Inoue, H. 1995, IAU Circ. 6241  
 Finger, M. H., Harmon, B. A., & Wilson, R. B. 1996a, ApJ, 459, 288  
 Finger, M. H., Wilson, R. B., Harmon, B. A., Hagedorn, K., & Prince, T. A. 1996b, IAU Circ. 6285  
 Fishman, G. J., et al. 1989, in Proc. Gamma Ray Observatory Science Workshop, ed. W. N. Johnson (Washington, DC: Naval Research Lab.), 2-39, 39  
 Giacconi, R., Gursky, H., Kellogg, E., Schreier, E., & Tananbaum, H. 1971, ApJ, 167, L67  
 Harmon, B. A., et al. 1991, The Compton Observatory Science Workshop (NASA CP-3137)  
 Koh, T., et al. 1995, IAU Circ. 6222  
 Lamb, F. K., Pethick, C. J., & Pines, D. 1973, ApJ, 224, 969  
 Motch, C., Janot-Pacheco, E., & Mouchet, M. 1991, ApJ, 369, 490  
 Nagase, F. 1989, PASJ, 41, 1  
 Parmar, A. N., White, N. E., Stella, L., Izzo, C., & Ferri, P. 1989, ApJ, 338, 359  
 Priedhorsky, W. C., & Holt, S. S. 1987, Space Sci. Rev., 45, 291  
 Stella, L., White, N. E., Davelaar, J., Parmar, A. N., Blissett, R. J., & van der Klis, M. 1985, ApJ, 288, L45  
 Stella, L., White, N. E., & Rosner, R. 1986, ApJ, 308, 669  
 Waters, L. B. F. M., & van Kerkwijk, M. H. 1989, A&A, 223, 196  
 Wilson, R. B., et al. 1993, AIP Conf. Proc. 304, The Second Compton Symposium, ed. C. E. Fichtel, N. Gehrels, & J. P. Norris (New York: AIP), 390  
 Wilson, R. B., Zhang, S. N., Scott, M., Harmon, B. A., Koh, T., Chakrabarty, D., Vaughan, B., & Prince, T. A. 1995b, IAU Circ. 6207  
 Zhang, S. N., Fishman, G. J., Harmon, B. A., & Paciesas, W. S. 1993, Nature, 366, 245